Journal of Carcinogenesis
Covering Genesis to Therapeutics

Journal of Carcinogenesis, ISSN: 1477-3163
2025; Vol 24: Issue 2, https://carcinogenesis.com/

Laser-Assisted Photothermal Therapy with Gold-Decorated Titanium Dioxide Nanotubes: A Cytotoxicity Evaluation in Colon Cancer Cells

Maher I. Al-Shemri[1], S. Z. Mortazavi[*2], M.R. Khanlary[1], Rana A. Ghaleb[3], A. Reyhani[1]

[1]Physics Department, Faculty of Science, Imam Khomeini International University, P.O. Box 34149-16818, Qazvin, Iran

[*2]Physics and Energy Engineering Department, Amirkabir University of Technology, P.O. Box 15875-4413, Tehran-Iran

[3]Department of Anatomy and Histology, College of Medicine, University of Babylon, Babylon, Iraq

***Corresponding Author:**

S. Z. Mortazavi

Email ID: z.mortazavi@aut.ac.ir

ABSTRACT

Au nanoparticles (NPs) successfully anchored on TiO_2 nanotubes (NTs) by electrochemical anodization method. The aim was to evaluate the efficiency of laser-assisted photothermal therapy using gold-decorated titanium dioxide nanotubes across varying doses and concentrations. Then, the survival of colon cancer cells (SW480) was tested in an environment with different concentrations of AuNPs decorated TiO_2 NTs with/without laser exposure at 532 and 808 nm in different times. A dose-dependent behavior was observed in cell viability of colon cancer cells treated with AuNPs-TiO_2 NTs under irradiation of laser. The effect depends on the concentration of nanoparticles, laser wavelength and the duration of laser irradiation. Specifically, infrared laser exposure (808nm) proved to be highly effective. In contrast, green laser exposure (532nm) showed only a minimal impact on cell survival. The findings collectively demonstrate that AuNPs-TiO_2 significantly impacts the viability of SW480 cancer cells, with the therapeutic effect being highly dependent on the concentration of nanoparticles and, critically, the wavelength and duration of laser irradiation, highlighting the superior efficacy of infrared light.

Keywords: *Cytotoxicity, Titanium Dioxide Nanotubes, Gold Nanostructures, Photothermal Therapy, Cancer Cells, Laser Light.*

How to Cite: Maher I. Al-Shemri, S. Z. Mortazavi, M.R. Khanlary, Rana A. Ghaleb, A. Reyhani, (2025) Laser-Assisted Photothermal Therapy with Gold-Decorated Titanium Dioxide Nanotubes: A Cytotoxicity Evaluation in Colon Cancer Cells, *Journal of Carcinogenesis*, *Vol.24, No.2*, 84-95

1. INTRODUCTION

Worldwide, cancer ranks high among the leading killers. Novel methods of cancer therapy are necessary due to the disease's status as a leading cause of death worldwide (Zhao et al., 2021). Due to the significant side effects of traditional cancer therapies like radiation and chemotherapy, researchers are continuously seeking more effective and painless treatment approaches. Photothermolysis has received a lot of attention from scientists all over the globe recently. A photoabsorbing substance is used in this method to destroy cancer cells by absorbing light of a certain wavelength and then releasing heat. Consequently, a reliable and risk-free light-absorbing material must be identified for this procedure. When paired with metal elements like gold, titanium dioxide nanoparticles can function as an effective photothermal agent, as they do not display any spectral bands in the near-infrared (NIR) region, which is where gold nanoparticles have a high light absorption band. In a 2014 study, Mehdizadeh et al. found that titania nanoparticles coated with gold, on the other hand, absorb light throughout a wide spectrum. Consequently, photothermolysis trials have a better chance of penetrating deep tissues and killing cancer cells selectively. (Beidu et al., 2023). One non-invasive approach to cancer treatment is phototherapy, which uses light energy conversion to heat in order to kill tumor cells (Bayazitoglu et al., 2013; Wu et al., 2020; Zhao et al., 2021). The photothermal agents (PTAs) and radiation penetration depth into the malignant tissue are the two most important factors that determine the efficacy of photothermal therapy (PTT) (Wu et al., 2020; Zhao et al., 2021). A novel approach to (photothermal) cancer treatment has recently attracted a lot of attention: titanium dioxide nanotubes (TNTs) covered

with gold nanostructures. A higher photothermal efficiency and improved PTA are both brought about by these nanostructures (Pisarek et al., 2021; Zhu et al., 2022). To ensure the safe application of this method, it is necessary to resolve the prevalent concern over the cytotoxicity of these nanostructures (Wang et al., 2015). This work aims to examine the toxicity of gold nanostructure-adorned titanium dioxide (TiO_2) nanotube arrays and assess their photothermal anticancer effect on colon cancer cells exposed to laser irradiation. In order to back up the findings, other investigations were conducted using tools such as X-ray diffraction (XRD), UV-Vis spectroscopy, among others. Through the conversion of laser light into heat and the selective destruction of cancer cells, the results demonstrate that gold-plated titanium dioxide nanotubes exhibit satisfactory performance in photothermolysis. Using nanostructures as PTA to treat cancer is an emerging field, and we think this study can shed fresh light on it.

2. MATERIALS AND METHODS

TiO_2 NTs were purchased from the Chinese company HW Nanomaterials, with a purity of 99% and a length greater than 1 micrometer. Then, electrochemical anodization method was also utilized to decorate gold nanoparticles on TiO_2 nanotubes. Accordingly, Au nanoparticles were anchored onto outer and inner parts of the NTs. Several analyses were applied to evaluate the samples. The morphology of the samples was explored using transmission electron microscope (TEM), with Philips, CM120. At first, a carbon-coated copper grid was coated using isopropanol suspension, and then the samples were dried in ambient conditions, and covered with a drop of 1% uranyl acetate, The filter paper was then used to absorb excess liquid from the grids before drying at ambient temperature. Furthermore, the FTIR spectra were taken at room temperature using a Perkin Elmer FTIR RX1 spectrometer. It was performed with IR Data Manager (IRDM) software. KBr discs containing TiO_2 and TiO_2@Au nanoparticles were prepared and dried in a vacuum oven. Furthermore, the X-ray diffraction patterns provided information on their crystalline size and behavior. The analysis was performed by a Philips PW1730 X-ray diffractometer operating at 0.15418 nm (CuKα radiation) wavelength. The analysis was performed by a Siemens D5000 X-ray diffractometer operating at 0.15418 nm (CuKα radiation) wavelength. In addition, the scattered waves were recorded in the range of 2θ from 10 to 90°. In addition, the UV-Visible absorption spectrum was obtained using the Shimadzu UV Vis Japan spectrophotometer equipped with Winlab UV software.

3. RESULTS AND DISCUSSION

TEM micrographs of the Au decorated TiO_2 NTs are illustrated in Fig. 1a and b, respectively. It is confirmed that the single-wall nanotubes are decorated by Au nanoparticles. The images show well-dispersed Au nanoparticles (dark contrast) on a TiO_2 NTs (lighter contrast). Some areas exhibit aggregation, where AuNPs appear clustered.

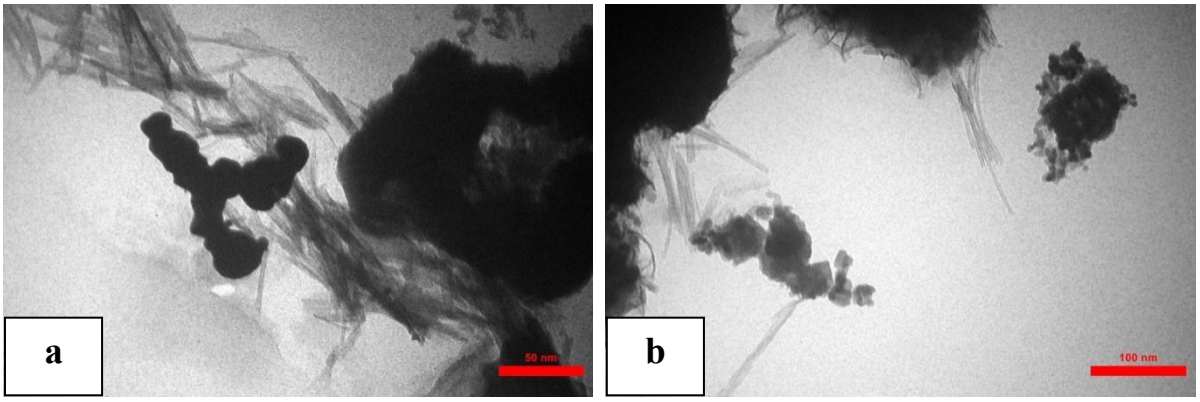

Fig. 1. TEM images of Au-decorated TiO_2 nanostructures.

Moreover, energy dispersive X-ray analysis (EDX) of the nanotubes is carried out and the corresponding data is tabulated in Table1. It shows the presence of titanium, oxygen, and gold elements. The atomic percentage of Au in the sample at 2.86 wt% confirms the anchoring of AuNPs on TiO_2 NTs.

Table 1. the corresponding EDX data of Au-decorated TiO_2 sample.

Element	Line Type	k Ratio	Wt%	Wt% Sigma	Atomic %
O	K series	0.01864	37.16	0.28	64.70
Ti	K series	0.14469	59.98	0.27	34.89
Au	M series	0.00576	2.86	0.17	0.41

Fig. 2 shows the FTIR spectrum of the sample in the range of 450–4000 cm^{-1} to identify the chemical bonds. The spectrum supports the successful synthesis of Au-decorated TiO_2 NTs, with expected Ti-O bands and additional surface functional groups. The peaks around 915 cm^{-1}, 755 cm^{-1}, 595 cm^{-1}, and 475 cm^{-1} correspond to the Ti-O and Ti-O-Ti stretching modes of the TiO_2 lattice. These peaks confirm the presence of TiO_2 as the main component of the sample. The decoration of TiO_2 with Au nanoparticles may cause slight shifts or changes in intensity of certain peaks, particularly in the low-frequency region (500-600 cm^{-1}). The interaction between Au and TiO_2 may enhance visible-light absorption and charge separation efficiency. FTIR shows shifts in Ti-O stretching peaks (~483 cm^{-1}, 475 cm^{-1}), suggesting interaction between Au and the TiO_2 lattice. The H-O-H bending peak (1630 cm^{-1}) also indicates adsorbed water, which may interact with Au, affecting photocatalytic properties. Moreover, the shifts in Ti-O vibrational peaks suggest Au modification of the TiO_2 lattice.

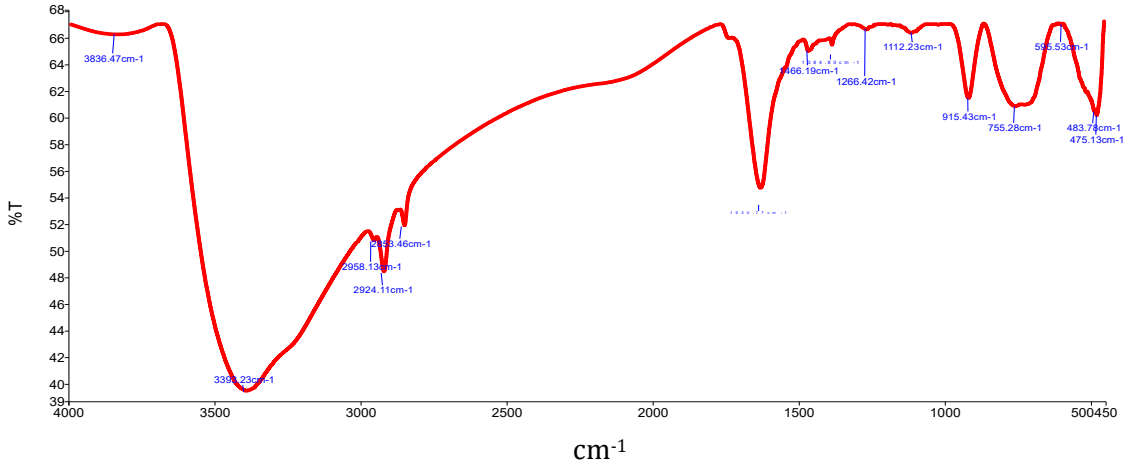

Fig. 2. FTIR spectrum of Au-decorated TiO_2 nanostructures

Fig. 3 depicts the XRD pattern of Au decorated TiO_2 NTs. The corresponding peaks of crystalline Au at 38.50°, 44.69°, 64.82°, and 77.78°. Furthermore, the peak at 25–28° is attributed to anatase or rutile of TiO_2.

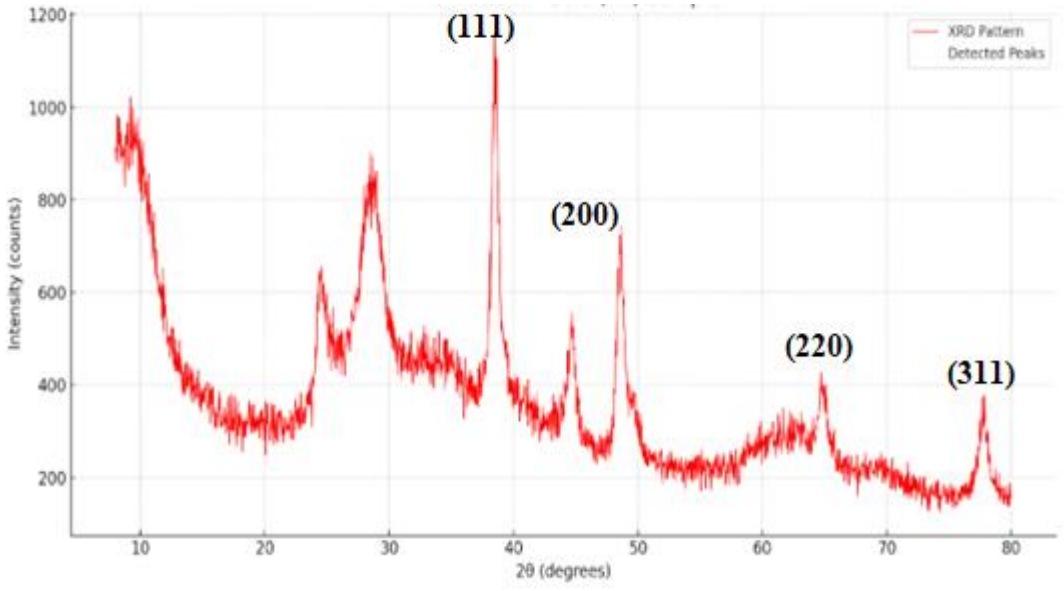

Fig. 3. X-ray diffraction pattern of Au-decorated TiO_2 nanostructures.

Moreover, Fig. 4 shows UV-Visible absorption spectrum which indicating the characteristic of TiO_2 NTs due to its intrinsic bandgap absorption (~3.2 eV for anatase TiO_2). A sharp decrease in absorption is observed beyond 350 nm, suggesting that the main absorption edge is due to the TiO_2 NTs. The presence of Au NPs modifies the absorption spectrum, introducing peaks in the visible range (400–600 nm). The inset shows additional features at 472 nm, 532 nm, and 610 nm,

which are likely due to the localized surface plasmon resonance (LSPR) of Au nanoparticles. The redshift towards 610 nm suggests the aggregation of Au nanoparticles which is in accordance with TEM images. The presence of AuNPs can shift or modify this absorption, indicating charge transfer between Au and TiO_2.

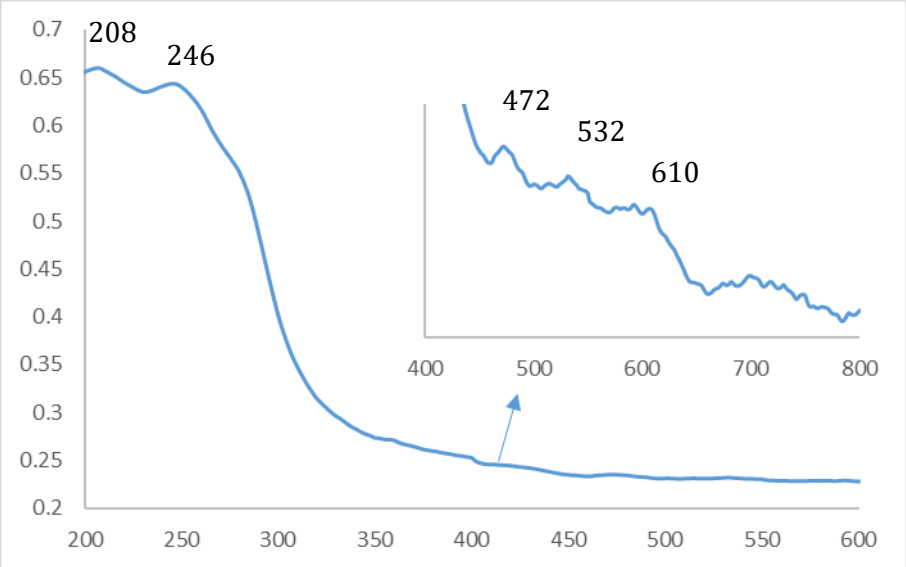

Fig. 4 . UV-Visible absorption spectrum of Au-decorated TiO_2 nanostructures.

Cell culture of Colon cancer

For preparation of serum-free culture medium, RPMI-1640-Powder was used to prepare the solution medium in accordance with the manufacturer´s recommendations (Gibco). In total 10.4 g of RPMI-1640 powder was dissolved in around 900 mL deionized distilled water (DDW) in a flask. The other things added include 2g of sodium bicarbonate powder and antibiotics. The components are added with continuous stirring. Then, deionized distilled water is added until the total volume reaches 1 liter. Under these conditions, the pH of the culture medium was 7.4. After that, the culture medium was sterilized using a graduated filter of (0.45 and 0.22 micrometer) filters and the culture medium was stored at a temperature of 4°C until use.

Furthermore, for preparation of serum culture medium, as explained previously, the serum culture medium was obtained by adding 10% of Fetal Bovine Serum (F.B.S). Then, 6 ml of serum-free culture medium, 1 ml of DMSO, and 3 ml of FBS serum, 10 ml of the frozen medium were prepared and then stored at -20°C.

1. Cell Thawing: The tube with frozen cells in liquid nitrogen is taken out and placed in a water bath at 37°C to dissolve ice. Before it melts completely, we take it out of water and sterilize it instantly with 70% ethanol, afterwards we take contents of this tube with cells inside the designated cabinet, then place them into a plastic box of 15 ml capacity. 10 ml is taken from the centrifuge containing the culture medium and added to it; thus, its rotational speed should be 800 rpm for a 10 min period. Afterwards, discard the liquid so that only cells will remain on bottom of the tube where other 5ml culture medium with 10% FBS is added. Finally moving them into another container having 25ml capacity which is shifted into an incubator maintained at 37°C and has its culture medium changed on next day.

2. Culturing Cell Lines: A common technique for handling monolayer cells attached to the bottom of culture vessels involves using the protein enzyme trypsin to dissociate and categorize them, primarily for multiplication and assessment purposes. This procedure is adapted when a substantial number of cells are required. The process begins by removing the culture medium before the cells reach their stationary growth phase and once they have formed a monolayer. Subsequently, the cells are washed with a warm Phosphate-Buffered Saline (PBS) solution. Approximately 3 ml of warm Trypsin-EDTA solution is then added to the tube containing the cells, ensuring it covers the monolayer during stirring, a step repeated 4-5 times to fully remove any residual liquid from the monolayer. To detach the single cell layer, the tube is incubated at 37°C. After incubation, the tube is removed and shaken to ensure complete cell separation. A graduated pipette is then used to suspend the cells, breaking up any clumps. Finally, the cells are dispersed in a growth medium containing 10% Fetal Bovine Serum (FBS) to neutralize the trypsin, with the exact percentage depending on the experimental requirements. These dissociated cells are then either grown in two layers or transferred to new tubes, depending on the specific experimental design.

Finally, in order to disperse TiO_2 nanotubes and TiO_2@Au into deionized water at a concentration of 1000µg/ml, first 0.1g of each sample were weighed and then disbursed using a digital sound device (Branson Ltd.). Next, these samples were

employed in the study of photodynamic therapy against colon cancer cells (SW480). The entire experiment was conducted using pure water of the Milli-Q type (Millipore, UK).

Design and Method of Cell Toxicity Test

During cell mortality phase, adherent cells are separated from cell culture plates, and this attribute is utilized to establish cell mortality. Another method for determining cell deaths is cell staining, which is a technique whereby there is detection of cell death through cell adhesion, where together with non-living ones, desired dye in proteins would make purple-colored living cells and those that have lost their attachment will be marked with purple color indicating their death. This indicates that if the number of purple colors decreased then such cells are regarded as dead or rather there are more dead cells than alive ones. This protocol serves as an assurance and explicit explanation on how to investigate and analyze effects of active compounds as well as chemotherapy agents on cell death. It should be noted that MTT analysis is usually employed for ascertainment of cytotoxicity or cytotoxicity of nanotubes and ascertainment of ordered death degree and survival degree of cultured cells. The cellular toxicity method is used in evaluating TiO_2 nanotubes and TiO_2@Au cytotoxicity by themselves and together with laser. In SW480 cell lines revolved low-energy laser treatment was done. Growth in monolayer Erlen was carried out before reaching the stationary phase; then the monolayer cell was harvested, distributed by growth medium and cultured in a diluted 96-well plate. Upon reaching 90% of cell growth six different concentrations of TiO_2 nanotubes and TiO_2@Au (500, 250, 125, 62.5, 31.25 and 15.6 µg/ml) were added to the channels and they were exposed to various laser devices with different irradiation times at different wavelengths and powers under dark conditions (Where all parameters tested were selected based on previous test results).

Using the mentioned materials, a purple-colored solution for crystal violet analyzer was prepared: 20 ml of methanol, 80 ml of distilled water, and 0.5 grams of crystal violet powder (Sigma Aldrich). To prepare the solution, the crystal violet powder is first dissolved in water and then methanol is added to it and then this solution is stored at room temperature and in the dark. The effectiveness of this solution reaches two months, and it should be used before that. After completing the designed experimental steps (cell culture, accumulation of nanotubes, laser irradiation, and incubation) to detect and verify cell death, the cultured cells were washed 3 times using 100 microliters of cold , then 100 microliters of crystal violet coloring solution was added to each house and incubated at a room temperature for 20 minutes.. Wash the plate three times in water with low flow and tilt the plate to prevent the water flow from directly colliding with the single cell layer (after filling the plate holes with water, the water must be immediately removed from the holes). After washing, the plate should be gently turned over on filter paper, to remove the remaining liquid, then the plate should be dried without a cover at room temperature for at least two hours. After that, using a 570-nm plate reader, the optical density of each house (cavity) is measured. The percentage of cellular toxicity and survival of cancer cells is calculated using the following relationships:

$$Viability\% = \frac{OD\ \ of\ \ test}{OD\ \ of\ \ control} \times 100$$

$$Cytotoxicity\% = 100\% - Viability\%$$

The difference between the optical density of the test wells and the optical density of the control group wells divided by the optical density of the control group is defined on the cell viability, and to calculate the percentage of viability it is enough to multiply this percentage by 100.

Laser irradiation of cells incubated with Au decorated TiO_2 NTs

A uniform irradiation lasted 24 hours on a 96-well plate containing cells. The laser light was delivered to one of the houses in a 96-houses plate (this distance was not. One of the ways to use in previous group research was this distance in laser irradiation). In this study three types of lasers with different outputs served as light sources, their characteristics are: 1. Continuous infrared laser with maximum output power of 150 mW and 808nm=808nm wavelength; 2. Continuous green laser having maximum output power at 300 mW and 532 nm wavelength. To calculate Fluency Energy Density (J/cm^2) for all treatment groups, we multiplied laser beam permeability (W/cm^2) by irradiation time. Also, we obtained the power density by dividing power over area. When growth occurs in a monolayer prior to attaining stationary phase, monolayer cells are detached using growth medium and diluted into a 96-well plate, then cultivated while cell growth attained 90% with different concentrations of TiO_2 nanotubes and TiO_2@Au being filled into the cavities at various l.

Furthermore, a cellular toxicity examination was carried out using laser therapy on SW480 colon cancer cell lines to study the poisonous effects of TiO_2@Au nanotubes. Infra Red laser (power = 150 mW; wavelength = 808 nm) was used in different fluorinesfluorine's with different energies for treating colon cancer cell lines SW480. Moreover, colon cancer cells (SW480) were also subjected to an experimental study for green laser (532 nm, 300 mw) . For the purpose of whether any toxicological consequences exist on normal cells or not, TiO_2 and TiO_2@Au nanotubules along with regular cells had been exposed to AuNPS**. Fig 6**

Study of the Effect of TiO_2 and Au@TiO2 Nanotubes on Cancer Cells

Utilizing three plates seeded at a density of 5×10^5, cancer cells were exposed to six concentration of Au@TiO2 nanotubes(500, 250, 125, 62.5 , 31.25 and 15.6 µg/ml) with three replicate for each one except for one column on every plate which served as control group. Moreover, after this,the plastic covers were put on the dishes and incubated for a period of 24 hours followed by an assessment of the cell line growth through evaluating cellular toxicity Crystal violet assay.

According to Fig. 5 All groups show a high percentage of cell viability (almost close to 100%) and it is clear that AuNPs decorated with TiO_2 at different concentrations have no significant cytotoxic effect on SW480 cells. Similar to some previous studies showing low toxicity of AuNP and TiO2 nanoparticles in cell types, our results also showed that these NPs had a high survival rate (Shahvardi et al., 2007; Park et al., 2008; Singh et al., 2013). What is more, some results demonstrate that AuNP and TiO2 nanoparticles are able to induce oxidative stress, DNA damage, apoptosis and inflammation in different cancer cells through size-, shape- surface charge-and coating dependent effects of the nanoparticles (Nel et al., 2006, Lanone and Boczkowski, 2006). Hence, the cell interaction of SW480 with AuNPs decorated TiO2 may rely on multiple factors which are still to be elucidated.

The non-cytotoxicity of decorated TiO2 nanoparticles may result from the point that these NPs could be restricted to access through SW480 cell membrane and then other inside body. The reason for this issue can be due to the reduction of the level and reactivity of nanoparticles accumulation due to the accumulation of nanoparticles in the culture medium (Schrand et al., 2010). On the other hand, SW480 cells may have high resistance or tolerance to TiO_2-decorated AuNPs, which could be related to their genetic or epigenetic characteristics, such as expression of multidrug resistance genes or antioxidant enzymes (Gottesman et al., 2002; Toyokuni , 2009). The validity of these possibilities can be checked by using different methods such as transmission electron microscopy, flow cytometry or gene expression analysis.

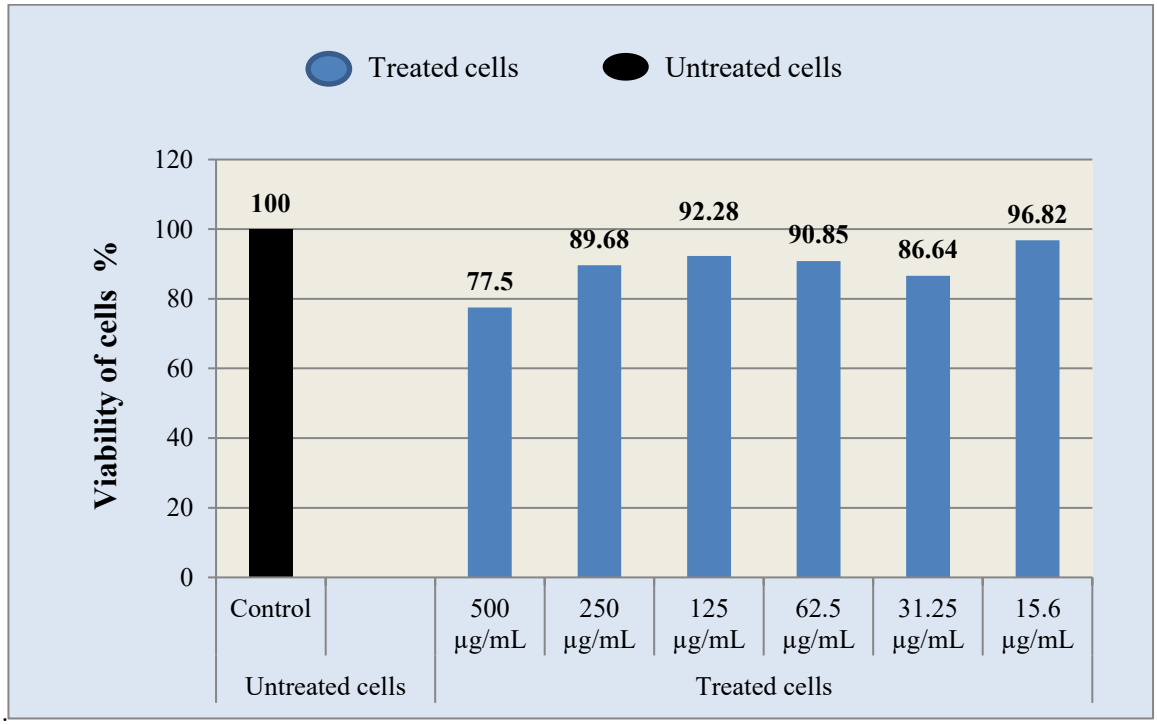

Fig. 5. Effect of AuNPs decorated TiO_2 on colon cancer cells (SW480 cells)

Effect of AuNPs Decorated TiO_2 on Colon Cancer Cells (SW480 Cells) after Exposed to 150 mw of 808 nm Infrared Laser for 1 min and 3 min respectively.

Fig. 6 displays the data concerning the viability of colon cancer cells (SW480 cells) that have undergone treatment with 150 mw of 808 nm Infrared laser for a period of 1 minute and 3 min respectively. . The cells were treated with varying concentrations of TiO_2 decorated AuNPs, and their viability was determined in comparison to an untreated control group of cells.

Viability of control cells: The untreated control cells displayed about 100% viability, suggesting that the infrared laser alone had little effect on the cells.

Viability of treated cells: At a concentration of 15.6 µg/ml, a slight decrease in the viability of treated cells was observed.

On the other hand, at higher concentrations, a significant decrease in cell viability was observed, which indicates a dose-response effect (31.25 µg/ml - 500 µg/ml). The lowest survival rate was reported at the concentration of 500 µg/ml with survival below 20%.

As seen in the results, AuNPs decorated with TiO2 had a significant effect on the destruction of SW480 colon cancer cells at a certain concentration under infrared laser irradiation. Existing studies showed that increasing the cellular uptake and light absorption of nanoparticles increases the potential of photothermal therapy in cancer treatment (Chen et al., 2016; Liu et al., 2018; Wang et al., 2019). Considering the increase in species production Reactive oxygen and thermal effects caused by the application of AuNP and infrared laser, the mechanism of cytotoxicity can be investigated (Huang et al., 2011; Liu et al., 2017; Li et al., 2018).

The cell viability is measured as a percentage of control, i.e., cells treated with no nanoparticles with the concentration of AuNPs decorated TiO_2 varying from 15.6 µg/ml - 500 µg/ml.

The findings show that using AuNPs decorated TiO_2 as a disposable treatment to develop infrared laser-based ablation therapy can produce a cytotoxic effect on SW480 cells. The cell viability decreases rapidly with exposure to all concentrations of AuNPs decorated TiO_2; however, at the maximum concentration, the cell viability reached only 10%. There are not observed differences in cell viability between the varying concentrations of AuNPs decorated TiO_2 implying even the minimum concentration can still elicit cell death.

Upon TiO_2 decorated with AuNPs can act as a light-thermal agent which heats the cancer cells subsequently as it converts light energy into thermal energy to damage the cancer cells (Wang et al., 2013). Besides, TiO_2 decorated with AuNPs may also produce reactive oxygen species (ROS) that will instigate oxidative stress and apoptosis in the cancer cells (Zhang et al., 2016). Whereas AuNPs decorated TiO_2 may have a specific affinity for the cancer cells. Thus, it plays a significant role in the development of nanoparticles (Li et al., 2017).) AuNPs decorated TiO_2 may give a new idea of the treatment of colon cancer by using the concept of advanced cancer therapy, which can be marginal to no toxicity, but still cure the patient. (Chen et al., 2018).

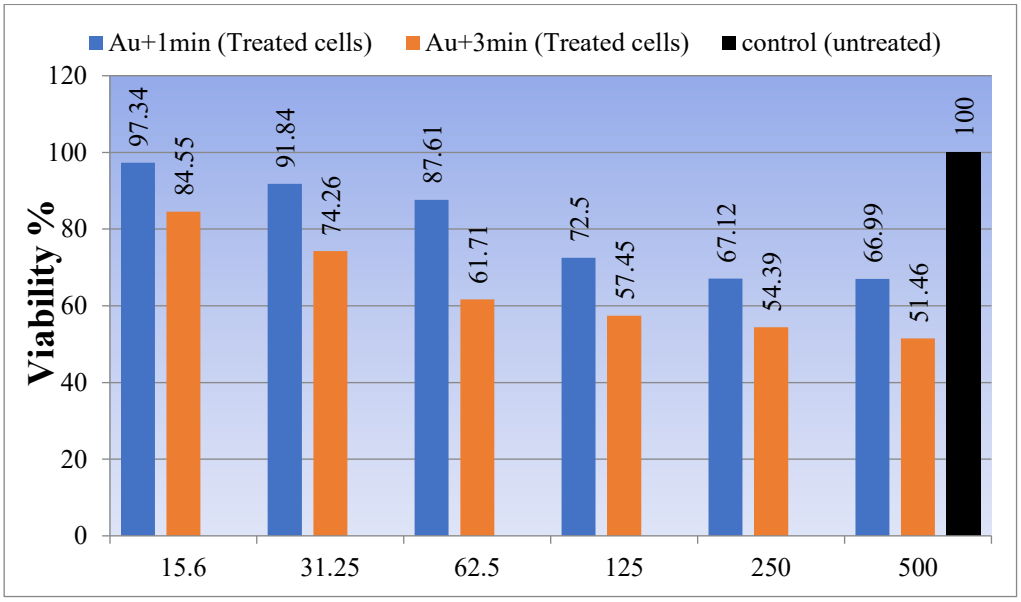

Fig. 6. Effect of AuNPs decorated TiO_2 on colon cancer cells (SW480 Cells)

Effect of AuNPs Decorated TiO_2 on Colon Cancer Cells (SW480 Cells) after Exposed to 150 mw of 532 nm Green Laser for 1 min and 3 min respectively.

Fig. 7 shows the application of different concentrations of TiO_2 decorated AuNPs for the treatment of colon cancer cells (SW480 cells) after exposure to 300 mW of 532 nm green laser for 1 minute and 3 min respectively. Then the results were compared with untreated control cells.

It can be clearly seen that cells treated with 500 µg/ml concentration showed approximately 82.86 and 72% viability, indicating a mild cytotoxic effect after exposed to 1 and 3 minutes green laser.

Obviously, TiO_2-decorated AuNPs have a significant effect on SW480 cancer cells under certain conditions. Therefore, it seems that TiO_2-decorated AuNPs can be used as a targeted therapy without damaging healthy tissues in be used around cancer cells.

Nonetheless, additional studies of the effect in varied concentrations of nanoparticles, laser beam exposure time and types of cancer cells are needed. Nanoparticles, under laser irradiation produces ROS that can increase oxidative stress and cause apoptosis in the cancer cells resulting into cell death as evidenced from their occurrence in literature. The mechanism of ROS production is concentration-dependent and can destroy cancer cells through the interaction of nanoparticles and light. At saturation level, on the other hand, cancer cells can produce or uptake ROS via one of numerous metabolic pathways. Furthermore, in the photothermal mechanism of action; nanoparticles absorb laser light which gets transformed to heat resulting thermal damage and necrosis remained on cancer cells. This can be explained overall according to nanoparticle state of aggregation, size and shape specific concentration dependence. On the other hand, the saturation point may occur due to thermal equilibrium between nanoparticles and cells.

The influence of AuNPs decorated TiO_2 with on the survival of Colon Cancer Cells (SW480) after illumination using 150 mw of green laser light at a wavelength of 532 nm for 3 minutes were shown in Fig. 7. From here, various dosages of AuNPs (ranging from 15.6 µg/ml - 500 µg/ml) were applied, then compared to the control condition of untreated cells. Cell viability was identified and quantitated as the ratio of cells survived to the number of the total cells. The viability of cells was not affected by gold nanoparticles (AuNPs) coated with titanium dioxide (TiO_2) at the given treatment. But further investigations must be done on different cancer cell lines, multiple concentrations of nanoparticles and varying periods of laser action.

It has been reported that nanoparticles can cause oxidative stress and apoptosis in the cancer cells via light-induced reactive oxygen species (ROS) production. This mechanism is concentration dependent and can lead to destruction of cancer cells due to interaction between nanoparticles and laser light, followed by ROS generation. Nevertheless, there is a limited possibility of ROS that will be saturated and ultimately involved in the regulation of bioenergy though various metabolic pathways. Moreover, a photothermal response is a process where laser light is absorbed by nanoparticles and then transferred into heat, which along with thermal damage and necrosis in the cancer cells, enables the photothermal effect to occur. Broadly speaking, the size, shape, and degree of nanoparticle aggregation are factors that explain the concentration-dependent effect.

Research in the field has already stated that the corresponding processes and the formation of reactive oxygen species (ROS) by nanoparticles because of the laser irradiation can invoke oxidative stress and apoptosis in cancer cells. The process can be realized by different concentrations which can destroy cancer cells by the way of the interactions of laser light with nanoparticles and ROS. Conversely, a certain quantity of ROS can be developed or absorbed via several different metabolic pathways at a saturation point. On the side, the photothermal effect is a procedure in which the laser light is trapped by the nanoparticles, and then it is transformed to heat thus during the heat process, thermal damage and necrosis occur the cancer cells. The concentration-dependent effect of nanoparticles someway depends on the size, shape, and aggregation state of the former ones.

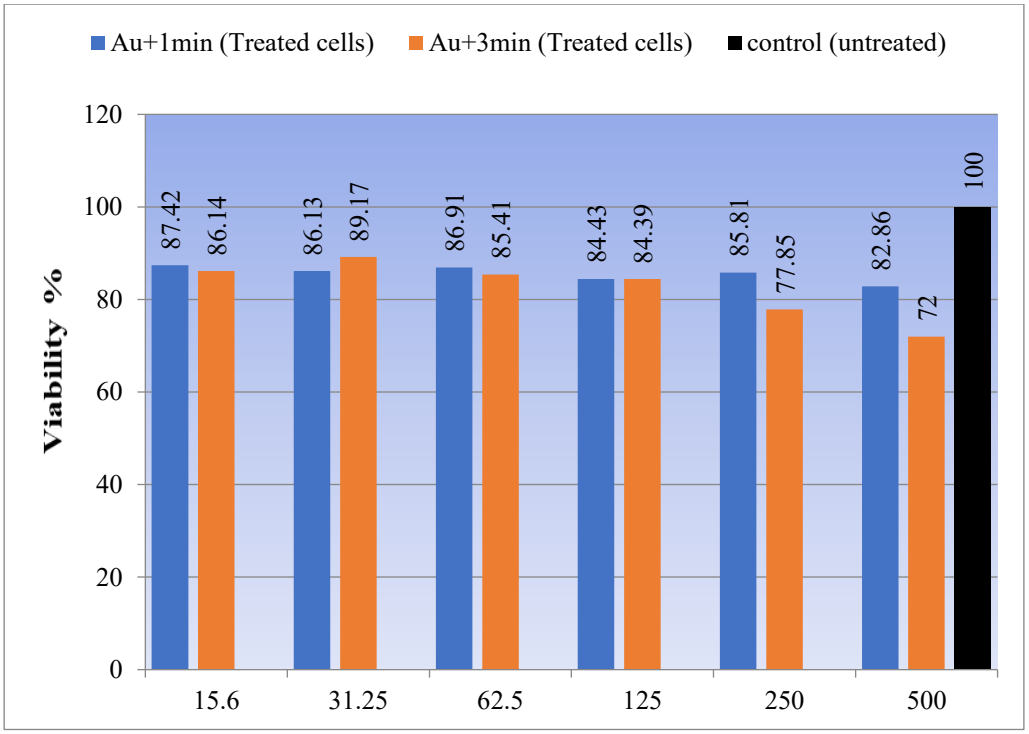

Fig. 7. Effect of AuNPs decorated TiO_2 on colon cancer cells (SW480 Cells)

In addition, the influence of AuNPs decorated TiO_2 with on the survival of Colon cancer cells (SW480) after exposed to 150 mw of 532 nm green laser and 808 nm infrared laser for 1 and 3 minutes were shown in Fig. 8 and 9, for comparison. In fact, AuNPs decorated TiO_2 NTs have a significant effect on the viability of SW480 cancer cells. A dose-dependent behavior was observed in cell viability of colon cancer cells treated with AuNPs-TiO_2 NTs under irradiation of infrared laser for 1 min; with minimal viability at 500 µg/ml. Moreover, at 3 min exposure, the survival of colon cancer cells decreased at all concentrations. The viability of colon cancer cells at 15.6 µg/ml was observed to be about 97.34%, regardless of concentration of nanoparticles, the survival of colon cancer cells was only slightly reduced. Additionally, exposure to green laser for 1 minutes, induced 82.86% colon cancer cell viability at concentrations of 500 µg/ml .

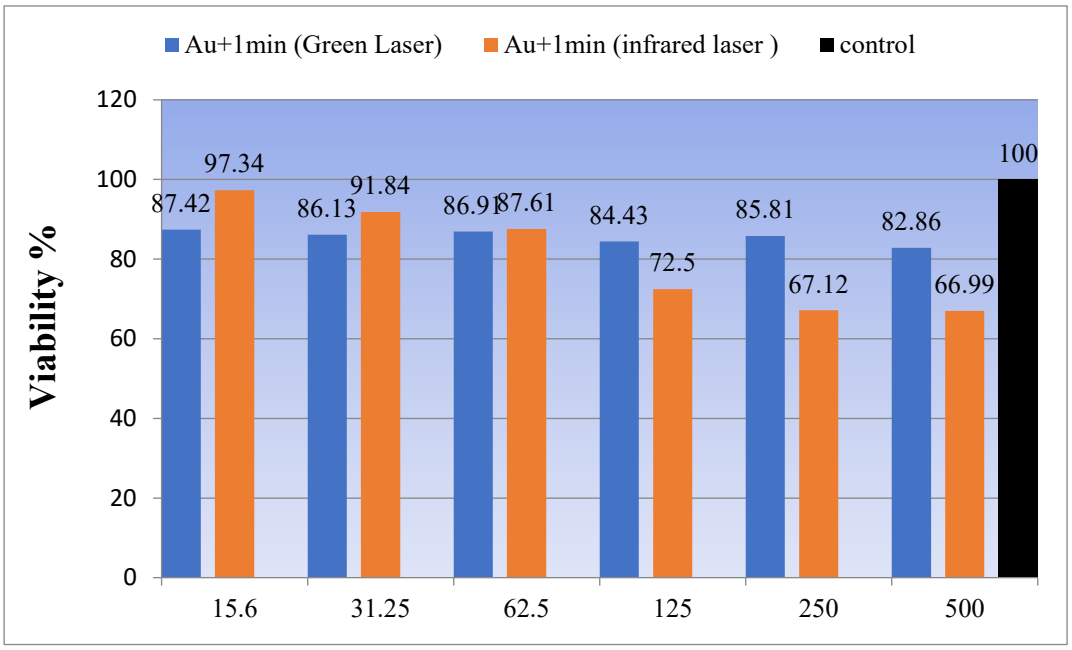

Fig. 8. Effect of AuNPs decorated TiO_2 on colon cancer cells (SW480 Cells) after exposed to 150 mw of 532 nm green laser and 808 nm infrared laser respectively for 1 min.

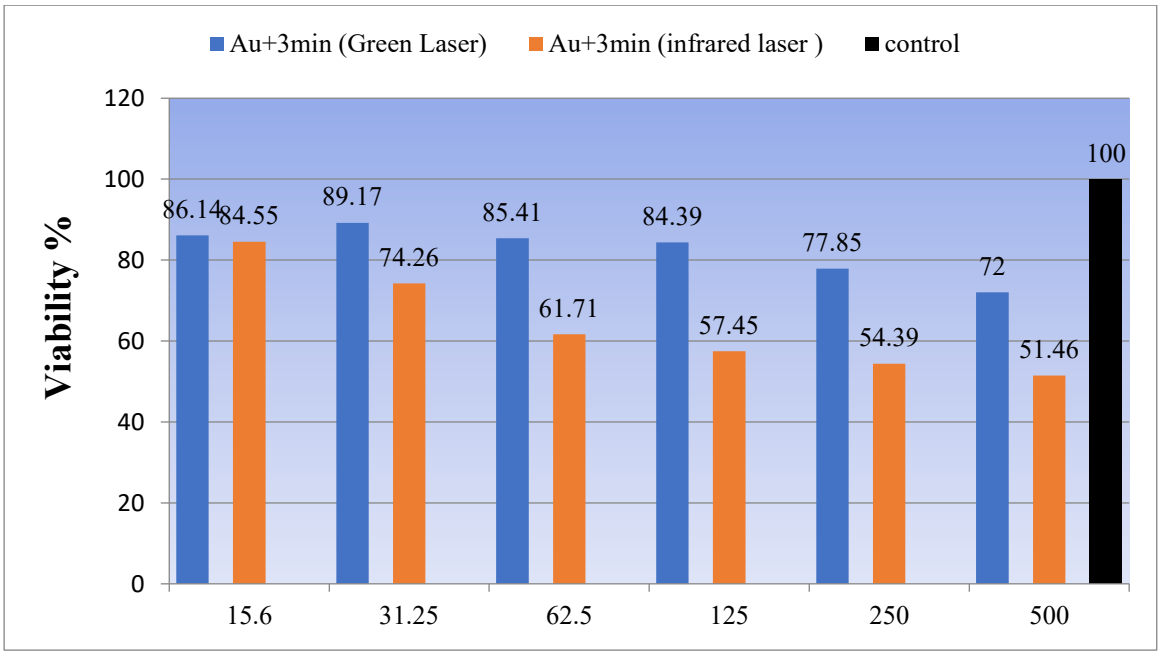

Fig. 9. Effect of AuNPs decorated TiO_2 on colon cancer cells (SW480 Cells)

In summary, the findings of this research demonstrate that varying concentrations of TiO_2-decorated AuNPs do not affect SW480 cell viability. Nevertheless, such a finding does not dismiss the possibility of TiO_2-decorated AuNPs being used in

cancer therapy as it may have other actions on cancer cells like changing proliferation, migration, invasion or angiogenesis. Moreover, radiation or phototherapy these systems may exhibit synergistic/additive properties. Therefore, additional studies are required to optimize synthesis, characterization and applications of these materials in cancer treatment.

4. CONCLUSIONS

It conclusively demonstrates that gold nanoparticles decorated on TiO_2 possess a significant ability to reduce the viability of SW480 colon cancer cells. Upon exposure to an 808 nm infrared (IR) laser, a significant dose-dependent reduction in cell viability was observed after 1 minute, with the lowest viability at 500 µg/ml. Extending the IR laser exposure to 3 minutes further decreased cancer cell survival across all tested concentrations, achieving optimal results at the increase of nanoparticle concentration. In contrast, irradiation with a 532 nm green laser for both 1 and 3 minutes resulted in only a marginal reduction in cell viability, remaining approximately 82.86 % for (1 min exposure) and 72% for (3 min exposure) at the higher concentrations of 500 µg/ml. It indicates a new approach to cancer treatment and reduce the damage to the healthy tissue around the colon cancer cells. The effectiveness of this photothermal approach is critically dependent on both the concentration of the nanoparticles and the characteristics of the laser irradiation. These findings underscore the potential of AuNPs−TiO_2 as a photothermal agent, particularly when activated by infrared light, for targeted cancer therapy, emphasizing the importance of optimizing both nanoparticle concentration and laser parameters for maximal therapeutic outcomes.

REFERENCES

[1] Akter, M., Atique Ullah, A. K. M., Banik, S., Sikder, M. T., Hosokawa, T., Saito, T., & Kurasaki, M. (2021). Green synthesized silver nanoparticles-mediated cytotoxic effect in colorectal cancer cells: NF-κB signal induced apoptosis through autophagy. Biological Trace Element Research, 199, 3272-3286.

[2] Althomali, A., Daghestani, M. H., Basil Almukaynizi, F., Al-Zahrani, S. A., Awad, M. A., Merghani, N. M., ... & Bhat, R. S. (2022). Anti-colon cancer activities of green-synthesized Moringa oleifera–AgNPs against human colon cancer cells. Green Processing and Synthesis, 11(1), 545-554.

[3] Amaroli, A., Sabbieti, M. G., Marchetti, L., Zekiy, A. O., Utyuzh, A. S., Marchegiani, A., ... & Agas, D. (2021). The effects of 808-nm near-infrared laser light irradiation on actin cytoskeleton reorganization in bone marrow mesenchymal stem cells. Cell and tissue research, 383, 1003-1016.

[4] Bao, J., Jiang, Z., Ding, W., Cao, Y., Yang, L., & Liu, J. (2022). Silver nanoparticles induce mitochondria-dependent apoptosis and late non-canonical autophagy in HT-29 colon cancer cells. Nanotechnology Reviews, 11(1), 1911-1926.

[5] Bayazitoglu, Y., Kheradmand, S., & Tullius, T. K. (2013). An overview of nanoparticle assisted laser therapy. International Journal of Heat and Mass Transfer, 67, 469-486.

[6] Chen, H., Zhang, X., Dai, S., Ma, Y., Cui, S., Achilefu, S., & Gu, Y. (2013). Multifunctional gold nanostar conjugates for tumor imaging and combined photothermal and chemo-therapy. Theranostics, 3(9), 633-649.

[7] Chen, Q., Xu, L., Liang, C., Wang, C., Peng, R., & Liu, Z. (2016). Photothermal therapy with immune-adjuvant nanoparticles together with checkpoint blockade for effective cancer immunotherapy. Nature communications, 7(1), 1-12.

[8] Chen, W., Zhang, J., Zhang, Z., Zhu, X., & Gu, N. (2013). Using chitosan–tripolyphosphate nanoparticles as a drug delivery system for targeting photodynamic therapy. Nanotechnology, 24(28), 285102.

[9] Chen, Y., Chen, H., Shi, J., & Chen, Z. (2018). Nanomaterials for photothermal therapy: current status and future perspective. Journal of hematology & oncology, 11(1), 1-17.

[10] Chen, Y., Chen, H., Zhang, S., Chen, F., Zhang, L., Zhang, Y., … & Liu, Y. (2014). Biosynthesis of silver nanoparticles by the endophytic fungus Epicoccum nigrum and their activity against pathogenic fungi. Bioprocess and biosystems engineering, 37(9), 1823-1829.

[11] Dheaa, D. J. and Mahdi, S. A. (2023). Photodynamic Therapy and TiO2-Decorated Ag Nanoparticles: Implications for Skin Cancer Treatment. Revue des Composites et des Matériaux Avancés-Journal of Composite and Advanced Materials, 33(6), 393-398.

[12] Duan, S., Hu, Y., Zhao, Y., Tang, K., Zhang, Z., Liu, Z., ... & Zhang, J. (2023). Nanomaterials for photothermal cancer therapy. RSC advances, 13(21), 14443-14460.

[13] Gottesman, M. M., Fojo, T., & Bates, S. E. (2002). Multidrug resistance in cancer: role of ATP–dependent transporters. Nature reviews cancer, 2(1), 48-58.

[14] Huang, X., El-Sayed, I. H., Qian, W., & El-Sayed, M. A. (2006). Cancer cell imaging and photothermal therapy in the near-infrared region by using gold nanorods. Journal of the American Chemical Society, 128(6), 2115-2120.

[15] Huang, X., Jain, P. K., El-Sayed, I. H., & El-Sayed, M. A. (2008). Plasmonic photothermal therapy (PPTT) using gold nanoparticles. Lasers in medical science, 23(3), 217-228.

[16] Huang, X., Li, L., Liu, T., Hao, N., Liu, H., Chen, D., & Tang, F. (2011). The shape effect of mesoporous silica nanoparticles on biodistribution, clearance, and biocompatibility in vivo. ACS nano, 5(7), 5390-5399.

[17] Lanone, S., & Boczkowski, J. (2006). Biomedical applications and potential health risks of nanomaterials: molecular mechanisms. Current molecular medicine, 6(6), 651-663.

[18] Li, J., Chen, Y., Guo, Z., Wang, C., & Li, C. (2017). Gold nanorods core/silver shell nanostructures integrated with optical coherence tomography and photoacoustic tomography for in vivo detection of colon cancer. Nanoscale, 9(20), 6788-6796.

[19] Li, X., Wang, L., Fan, Y., Feng, Q., & Cui, F. Z. (2010). Biocompatibility and toxicity of nanoparticles and nanotubes. Journal of nanomaterials, 2010.

[20] Liu, Y., Ai, K., Yuan, Q., & Lu, L. (2011). Fluorescence-enhanced gadolinium-doped zinc oxide quantum dots for magnetic resonance and fluorescence imaging. Biomaterials, 32(4), 1185-1192.

[21] Liu, Y., Crawford, B. M., & Vo-Dinh, T. (2018). Gold nanoparticles-mediated photothermal therapy and immunotherapy. Immunotherapy, 10(13), 1175-1188.

[22] Liu, Y., et al. (2017). Recent progress in surface modification of magnetic iron oxide nanoparticles for biomedical applications. Journal of Materials Chemistry B, 5(46), 9108-9124.

[23] Liu, Y., et al. (2018). Recent advances in NIR-responsive photothermal therapy nanosystems. Nanoscale, 10(46), 21609-21625.

[24] Mehdizadeh, A., Pandesh, S., Shakeri-Zadeh, A., Kamrava, S. K., Habib-Agahi, M., Farhadi, M., Pishghadam, M., Ahmadi, A., Arami, S., & Fedutik, Y. (2014). The effects of folate-conjugated gold nanorods in combination with plasmonic photothermal therapy on mouth epidermal carcinoma cells. [PDF]

[25] Mitu, S. A., Ahmed, K., Bui, F. M., Chen, L., Smirani, L. K., Patel, S. K., & Sorathiya, V. (2023). Au-TiO2-Coated Spectroscopy-Based Human Teeth Disorder Detection Sensor: Design and Quantitative Analysis. Micromachines, 14(6), 1191. mdpi.com

[26] Narasimha, V. R., Latha, T. S., Pallu, R., Panati, K. and Narala, V. R. (2022). Anticancer activities of biogenic silver nanoparticles targeting apoptosis and inflammatory pathways in colon cancer cells. Journal of Cluster Science, 33(5), 2215-2231.

[27] Nel, A., Xia, T., Madler, L., & Li, N. (2006). Toxic potential of materials at the nanolevel. science, 311(5761), 622-627.

[28] Park, J. H., Lee, S., Kim, J. H., Park, K., Kim, K., & Kwon, I. C. (2008). Polymeric nanomedicine for cancer therapy. Progress in polymer science, 33(1), 113-137.

[29] Pisarek, M., Krawczyk, M., Kosiński, A., Hołdyński, M., Andrzejczuk, M., Krajczewski, J., ... & Lisowski, W. (2021). Materials characterization of TiO 2 nanotubes decorated by Au nanoparticles for photoelectrochemical applications. RSC advances, 11(61), 38727-38738.

[30] Schrand, A. M., Rahman, M. F., Hussain, S. M., Schlager, J. J., Smith, D. A., & Syed, A. F. (2010). Metal-based nanoparticles and their toxicity assessment. Wiley interdisciplinary reviews: Nanomedicine and Nanobiotechnology, 2(5), 544-568.

[31] Shahverdi, A. R., Fakhimi, A., Shahverdi, H. R., & Minaian, S. (2007). Synthesis and effect of silver nanoparticles on the antibacterial activity of different antibiotics against Staphylococcus aureus and Escherichia coli. Nanomedicine: Nanotechnology, Biology and Medicine, 3(2), 168-171.

[32] Singh, S. K., Goswami, A., & Sharma, A. K. (2013). Biomedical applications of TiO2 nanoparticles: An overview. Nanotechnology Reviews, 2(6), 639-649.

[33] Soenen, S. J., Himmelreich, U., Nuytten, N., & De Cuyper, M. (2011). Cytotoxic effects of iron oxide nanoparticles and implications for safety in cell labelling. Biomaterials, 32(1), 195-205.

[34] Toyokuni, S. (2009). Role of iron in carcinogenesis: cancer as a ferrotoxic disease. Cancer science, 100(1), 9-16.

[35] Wang, C., Tao, H., Cheng, L., & Liu, Z. (2011). Near-infrared light induced in vivo photodynamic therapy of cancer based on upconversion nanoparticles. Biomaterials, 32(26), 6145-6154.

[36] Wang, X., et al. (2019). Gold nanoparticles decorated TiO2 nanotubes for enhanced photothermal therapy of cancer. Nanomaterials, 9(2), 213.

[37] Wang, X., Liu, K., Yang, G., Cheng, L., He, L., Liu, Y., … & Liu, Z. (2013). Near-infrared light triggered photodynamic therapy in combination with gene therapy using upconversion nanoparticles for effective

cancer cell killing. Nanoscale, 5(15), 6702-6710.

[38] Wang, X., Liu, Y., Li, Y. and Wang, H. (2016). Silver nanoparticles sensitize titanium dioxide for enhanced photocatalytic activity under visible light irradiation. Journal of Nanoparticle Research, 18(1), 1-9.

[39] Wang, Y., Cui, H., Zhou, J., Li, F., Wang, J., Chen, M., & Liu, Q. (2015). Cytotoxicity, DNA damage, and apoptosis induced by titanium dioxide nanoparticles in human non-small cell lung cancer A549 cells. Environmental Science and Pollution Research, 22, 5519-5530.

[40] Wu, X., Suo, Y., Shi, H., Liu, R., Wu, F., Wang, T., ... & Cheng, Z. (2020). Deep-tissue photothermal therapy using laser illumination at NIR-IIa window. Nano-Micro Letters, 12, 1-13.

[41] Zhang, Y., Wang, J., Xu, L., Wang, E. and Li, Z. (2010). In vitro and in vivo activities of Ag-TiO2 nanocomposite on osteosarcoma. Biomaterials, 31(22), 5807-5815.

[42] Zhang, Y., Wang, X., Wang, C., Li, Z., Hu, J., & Zhang, X. (2016). Au@ TiO2 core–shell nanoparticles for improved photodynamic therapy and chemotherapy against colon cancer. ACS applied materials & interfaces, 8(32), 20715-20722.

[43] Zhang, Y., Wang, Y., Wang, L., Jiang, X., & Li, X. (2016). Ag/TiO2 nanocomposite as a highly efficient visible light responsive photocatalyst: effects of silver content, calcination temperature and crystal structure. Applied Surface Science, 387, 66-76.

[44] Zhao, L., Zhang, X., Wang, X., Guan, X., Zhang, W., & Ma, J. (2021). Recent advances in selective photothermal therapy of tumor. Journal of nanobiotechnology, 19, 1-15.

[45] Zhu, H., Tan, J., Qiu, J., Wang, D., Zhao, Z., Lu, Z., ... & Mei, Y. (2022). Gold nanoparticles decorated titanium oxide nanotubes with enhanced antibacterial activity driven by photocatalytic memory effect. Coatings, 12(9), 1351.